High throughput process development for the purification of rapeseed proteins napin and cruciferin by ion exchange chromatography

Moreno-González, Mónica; Chuekitkumchorn, Pattra; Silva, Marcelo; Groenewoud, Roos; Ottens, Marcel

DOI
10.1016/j.fbp.2020.11.011

Publication date
2021

Document Version
Final published version

Published in
Food and Bioproducts Processing

Contents lists available at ScienceDirect

Food and Bioproducts Processing

journal homepage: www.elsevier.com/locate/fbp

High throughput process development for the purification of rapeseed proteins napin and cruciferin by ion exchange chromatography

*Mónica Moreno-González, Pattra Chuekitkumchorn, Marcelo Silva, Roos Groenewoud, Marcel Ottens**

Department of Biotechnology, Delft University of Technology, van der Maasweg 9, 2629 HZ Delft, the Netherlands

ARTICLE INFO

Article history:
Received 26 May 2020
Received in revised form 9 November 2020
Accepted 22 November 2020
Available online 30 November 2020

Keywords:
Canola meal proteins
High throughput experimentation
Chromatography
Ion Exchange
Column simulation

ABSTRACT

Proteins derived from plant resources such as oilseed meals, canola and sunflower, are considered a viable alternative to animal proteins for food consumption. This work presents a rational methodology, using high throughput experimentation (HTE), for the separation of cruciferin and napin, the two major proteins of canola meal, by chromatography. Eight different mixed mode and ion exchange resins were evaluated at different conditions with the aim of capturing napin and identifying adsorption/desorption behavior, ease of desorption and selectivity. POROS 50 HS resulted as the most promising resin. The obtained equilibrium adsorption data for napin and cruciferin was used in a mechanistic chromatography model and compared with experimental results showing a very good agreement. The model was used to identify column operating parameters that lead to >98% yield and purity for both proteins. Subsequently a conceptual downstream processing was proposed.

1. Introduction

Global protein demand has risen as a result of growing population and in order to satisfy this demand protein with appropriate quality needs to be generated from animal and plant sources (Wanasundara et al., 2016). Valorization of agri-food byproducts, such as oilseed meal, could help to satisfy the demand of the future food supply across the world. Canola meal is a competitive plant-based protein source, it contains ~40% protein content; ~12 % of crude fiber, 3% phenolic compounds and 3% of phytic acid among others (Lomascolo et al., 2012; Wanasundara, 2011; Wanasundara et al., 2017). Proteins from this meal have potential applications in bakery products as emulsifiers, in diary and dressing products as egg white protein replacement (Kodagoda et al., 1973), in beverages as protein supplement, meat binders, mayonnaise and in cheese-like products (Wanasundara et al., 2016). Moreover, canola proteins are reported to have antiamnestic, anti-oxidative, antihypertensive, anorectic and antithrombotic properties (Wanasundara, 2011; Wanasundara et al., 2016).

Napin and cruciferin are the two major proteins in canola meal, these are storage proteins with different characteristics. Napin (2S albumin) is a basic protein with an isoelectric point around 11 and a molecular weight between 12-14 kDa. Highly soluble in water at a wide pH range, stable at high temperatures (75 °C) (Jyothi et al., 2007; Perera et al., 2016) and holds foaming properties (Aider and Barbana, 2011; Schmidt et al., 2004; Wanasundara et al., 2016a). Napin protein constitutes around 20% of the protein content of canola meal, while cruciferin represent 60% (Wanasundara, 2011). Cruciferin (11S globulin) has an isoelectric point of around 7.2 and a molecular weight between 230–300 kDa, much higher than napin protein. This protein resembles structural features of other seed storage proteins (Adachi et al., 2003) and has well organized structural levels (Wanasundara et al., 2017). In contrast with napin, cruciferin possesses gelling, binding and emulsi-

* Corresponding author.
E-mail address: M.Ottens@tudelft.nl (M. Ottens).

https://doi.org/10.1016/j.fbp.2020.11.011

fying properties which makes it an interesting product for food applications (Aider and Barbana, 2011; Wanasundara, 2011).

Several methods have been described to successfully extract proteins from defatted oilseed meals including solvent extraction, aqueous and alkaline extraction assisted with salt and enzymes. The reported protein yields vary between 50% and 80% (Contreras et al., 2019; Fetzer et al., 2018; Pickardt et al., 2009; Vuorela et al., 2004). Despite the high protein level in canola meal extracts, the presence of glucosinolates, phytic acid and phenolics, which are also co-extracted, could limit application of the proteins in food products. Therefore, effective separation techniques such as membrane processes (Akbari and Wu, 2015; Ghodsvali et al., 2005; Xu and Diosady, 2002) are required for the separation of such antinutritional components (Wanasundara et al., 2017). Even though phenolics are considered antinutritional components, their recovery might present some economic potential. Given their antioxidative properties, they have potential application in the fields of cosmetics, pharmaceutical and food products (Moreno-González et al., 2020).

Purification of the extracted proteins can be accomplished by several methods such as isoelectric precipitation followed by membrane separation (Ghodsvali et al., 2005; Xu and Diosady, 2002) and protein micellar formation (Murray et al., 1980), being isoelectric precipitation (after alkaline extraction) the most applied. However, extreme alkaline conditions can have a negative effect on the functionality of the proteins due to denaturalization, loss of essential amino acids and lysinoalanine formation (Fetzer et al., 2018; Gerzhova et al., 2015; Hou et al., 2017; Rommi et al., 2015). In addition, high pH might create protein-polyphenols complexes, which make protein products dark and have bitter flavor. Similarly, protein precipitation might reduce the solubility of products and promotes protein denaturation caused by globulin aggregates (Bérot et al., 2005; Raab and Schwenke, 1984). Moreover, co-precipitation of both proteins might occur leading to protein mixtures rather than individual protein isolates. Application of more selective and milder conditions, such as aqueous extraction and chromatography could be applied to keep protein functionality and improve purity of each protein product. Studies in purification of canola proteins by chromatography have been evaluated (Bérot et al., 2005; Pudel et al., 2015; Zhang et al., 2007) using cation exchange resins (CEX), hydrophobic interaction (HIC) and size exclusion (SEC), showing the promising potential of applying this technology.

This study presents a rational strategy for the separation of cruciferin and napin proteins from canola meal extract by preparative protein chromatography. Protein extraction is assumed to be done at pH6 and at 0.3 M NaCl. The strategy involves the evaluation of different cation exchange resins (CaptoS, POROS 50HS, CM Sheparose and MacroPrep 50) and mixed mode resins (CaptoMMC, Nuvia cPrime, PPA HyperCel and Toyopearl MX-Trp-650 M) at different pH values and salt concentrations to identify adsorption/desorption conditions with the goal of capturing napin. Resin screening was done by means of high throughput experimentation (HTE) Additionally, resin selection was done by establishing a resin selection criteria based on napin capacity, selectivity, ease of desorption and resin price. The obtained equilibrium information was used in a column adsorption/desorption model which is then used to suggest a conceptual downstream process for the separation of the two major proteins (cruciferin and napin) from canola meal extract.

2. Materials and methods

2.1. Chemicals

For preparation of the buffers and solutions analytical grade chemicals were used. Bis-tris (>98%), tris-HCl (>98%), acetonitrile (HPLC grade), hydrochloric acid analytical reagent (37%), trifluoroacetic acid (>99%) were obtained from Sigma-Aldrich, the Netherlands. Sodium chloride (>99%) was purchased from J.T. Baker, Denmark, sodium hydroxide from Mallinckrodt Baker, The Netherlands, and Ethanol: Emsure absolute for analysis was obtained from Merck, The Netherlands.

The used proteins are: napin isolate (>98%, ABIN1995012), cruciferin isolate (>98%, ABIN1995013) and rapeseed protein mixture (57% napin and 43% cruciferin, ABIN1995014). The products were acquired from antibodies-online, GmbH, Germany. As cruciferin isolate presented very limited solubility properties in water, it was decided to use the rapeseed protein mixture to perform binary adsorption experiments.

Napin isolate, cruciferin isolate and rapeseed protein mixture were characterized by SDS-PAGE under non-reducing conditions and reducing conditions (reducing agent TCEP solution). SDS-PAGE was performed on a 4–12% Bis-Tris Gel (NuPAGE™ Novex) at constant voltage (200 V). The non-reduced sample was prepared with NuPAGE™ LDS sample buffer. The reduced sample was incubated with LDS sample buffer before loading on gel. NuPAGE Mark12™ was used as a molecular marker. The electrophoresis was carried out using MES SDS as running buffer. After running, the gel was stained in GelCode™ Blue Safe Protein Stain and destained with Milli-Q water. All SDS-PAGE reagents were obtained from ThermoScientific, The Netherlands.

2.2. Resins

Three mixed mode cation resins: Capto MMC (GE Healthcare, Sweden), Nuvia cPrime (Bio Rad, USA) and Toyopearl MX-Trp-650 M (Tosoh, Japan); one mixed mode anion resin, PPA HyperCel (Pall Life Sciences, France), two strong cation resins, Capto S (GE Healthcare, Sweden) and POROS 50HS (ThermoFisher Scientific, The Netherlands) and two weak cation resins, CM Sepharose Fastflow (GE Healthcare, Sweden) and MacroPrep50 CM (Bio Rad, USA), were used to evaluate napin and cruciferin adsorption. The characteristics of all resins are shown in Table 1.

2.3. Buffer solution and preparations

For buffers at pH 4, pH 5, pH 6 and pH 8, lactic acid, acetic acid, bis-tris and tris-HCl were used respectively. All buffers were prepared by dissolving the amount of salt corresponding to 50 mM in Milli-Q water, adjusting the pH using 2 M HCl or 2 M NaOH. The salt concentration was adjusted to 0.1 M, 0.3 M, 0.7 M and 1.0 M by adding the corresponding amount of NaCl before completing buffer final volume. All buffers were filtered previous to use using filters with 0.45 μm pore size.

Napin stock solution was prepared by dissolving napin protein (8 g/L) in the appropriate buffer and filtered with a disposable 0.22 μm PVDF filter. This napin stock solution was diluted to different napin concentrations (from 1 to 8 g/L) using Milli-Q water.

In binary component experiments, protein mixture (napin + cruciferin) was dissolved in the corresponding buffer.

Table 1 – Mixed mode and Ion exchange resins.

Name/Type		pKa	Matrix composition[a]	Ligand density[a] (mmol/L) [a]
Capto MMC	Mixed mode weak cation exchanger	~4.6[b]	Highly cross-linked agarose	80
Nuvia cPrime	Mixed mode weak cation exchanger	~4.5[b]	Macroporous highly cross-linked hydrophilic polymer	65
Toyopearl MX-Trp-650 M	Mixed mode weak cation exchanger	2.9 and 9.4[c]	Methacrylic polymer matrix	110
PPA HyperCel	Weak anion exchanger	8	High porosity cross-linked cellulose	65
Capto S	Strong cation exchanger	1.2	Highly cross-linked agarose with dextran surface extender	125
POROS 50 HS	Strong cation exchanger	1.2	Cross-linked polystyrene-divinylbenzene	104
CM Sepharose Fastflow	Weak cation exchanger	4.7	Cross-linked agarose	80
MacroPrep50 CM	Weak cation exchanger	4.7	Methacrylate polymer based	210

[a] Provided by resin suppliers.
[b] Based on (Zhu and Carta, 2016).
[c] Based on the pKa of the tryptophan ligand (National Center for Biotechnology Information, 2020).

The solution was sonicated at room temperature for 30 min in order to increase the solubility of cruciferin. After that, insolubilized protein was removed by filtering with a disposable 0.22 μm PVDF filter, this stock solution was diluted to evaluate cruciferin effect on napin adsorption.

2.4. Analytical methods

In single component napin experiments, the concentration of the protein was measured spectrophotometrically, measuring the absorbance at 280 nm using the spectrophotometer InfiniTe Pro 200 plate reader (Tecan, Switzerland). The measurement was performed with 100 μL of liquid solution in a 96-well half-area microplate (UV-STAR®, Greiner bio-one, Germany)

To measure the concentration of both proteins, in the protein mixture experiments, reverse phase liquid chromatography (RPC) was applied. The analysis was done using an Ultra High Performance Liquid Chromatography system (UHPLC Ultimate 3000) (Thermo Scientific, USA) equipped with a Zorbax 300 SB-C8 Rapid Resolution HD column (2.1 × 100 mm, 1.8 μm) (Agilent, USA). The column was equilibrated with 20% acetonitrile supplemented with 0.1% Trifluoroacetic acid (TFA) at 0.3 mL/min keeping column temperature at 30°C. The sample was injected and a gradient of acetonitrile started from 20% to 75% in 7 min, detection was done at 280 nm. Then the column was washed with 75% acetonitrile supplemented with 0.1% TFA for 5 min before the next injection. Napin calibration lines were evaluated using napin protein isolate. Since cruciferin isolate did not show the expected characteristics, as the polypeptide profile did not show the corresponding bands (Supplementary material), a standard curve could not be obtained. The relative change of concentration was used to evaluate cruciferin. Assuming that the ratio between equilibrium concentration and initial concentration is proportional to peak area ratio $\left(\frac{C_e}{C_{feed}} = \frac{Area\ peak\ after\ adsoprtion}{Area\ peak\ of\ feed}\right)$ determined by UHPLC.

2.5. Batch adsorption experiments

Batch experiments were performed in order to determine adsorption equilibrium isotherms of napin and cruciferin at different adsorption/desorption conditions on different mixed mode and ion exchange resins, in order to separate both proteins.

2.5.1. Adsorption equilibrium isotherms

Napin adsorption equilibrium isotherms were evaluated using a Tecan EVO Freedom 200 robotic station (Tecan, Switzerland) equipped with an orbital mixer (Te-shake), an automated vacuum system (Te-VacS), a plate reader (InfiniTe Pro 200), a robotic manipulator (RoMa) arm (to move microplates to the different positions of the robotic station) and two liquid handing arms (LiHa and MCA96). The procedure involves the different steps of the chromatography run until adsorption (washing, equilibration and adsorption). A known amount of each resin (15.6 μL or 23.4 μL) was added to the wells of a 96 deep-well filter plate (catalog number: MDRLN0410) from Millipore, USA. Resins were added using MediaScout® ResiQuot resin loader (Atoll, Germany). Resin were washed two times with Milli-Q water using the vacuum system (Te-VacS) and equilibrated with the corresponding buffer for 20 min. under agitation (1200 rpm). Equilibration buffer was removed by centrifugation with an Eppendorf centrifuge 5810 R (rotation speed 4000 rpm for 3 min). After centrifugation, resins were contacted with 312 μL of napin solutions under agitation until equilibrium was reached (2 h at 1200 rpm). Once equilibrium was reached, the filter plate was centrifuged to collect the supernatant and equilibrium concentration was measured spectrophotometrically (see 2.4 Analytical methods). Napin experiments were performed in duplicate.

Effect of pH and ionic strength were evaluated for napin adsorption by performing experiments at 4 different pH (pH 4, 5, 6, 8) keeping NaCl concentration (0.3 M) constant and at pH 6 varying salt concentration from 0.1 M to 1 M NaCl. This allows to identify desorption conditions.

Napin adsorption capacity was calculated according to the mass balance Eq. (1)

$$q_{p,eq} = \frac{C_{p,load} * V_{load} - C_{p,eq}\,(V_H + V_{load})}{V_{resin}} \quad (1)$$

Where $q_{p,eq}$ is the adsorption capacity (mg/mL$_{resin}$), $C_{p,load}$ is the protein initial concentration (mg/mL), V_{load} is volume of the liquid phase (mL) $C_{p,eq}$ is the protein equilibrium concentration (mg/mL), V_H is the holdup volume (mL) and V_{resin} is the volume of resin (mL).

After centrifugation, some liquid could remain in the resin. This liquid holdup was determined using the method suggested by Nfor et al. (2010). The resins were placed in a deep-well filter plate and equilibrated with 350 μL of 1 M NaCl. After 45 min the filter plate was centrifuged with 5810 R centrifuge (Eppendorf, Germany) for 3 min at 4000 rpm and the flow through was collected to measure conductivity. This cycle was repeated until the conductivity of flow through was equal to the conductivity of 1 M NaCl solution. Consequently, the equilibrated resins were contacted with 312 μL of Milli-Q water and incubated overnight without agitation. After contacting, the filter plate was centrifuged and the conductivity of the flow-through was measured. All the conditions were done in triplicate. The conductivity was measured with a multiparameter analyzer C832 (Consort NV, Belgium).

The holdup volume was measured using the salt mass balance Eq. (2)

$$C_{S,initial} * V_H = C_{S,final} * (V_H + V_W) \quad (2)$$

Initial salt concentration in all resins was 1 M NaCl ($C_{S,initial}$), V_H is holdup volume (mL), $C_{S,final}$ is the final salt concentration after contacting with Milli-Q water and V_W is the added volume of Milli-Q water.

Since cruciferin has low solubility in water, cruciferin adsorption isotherms were evaluated using the protein mixture. A similar procedure to the one applied for napin adsorption isotherms was used with the protein mixture in the liquid handling robotic station. The evaluated conditions were: pH 6 and 0.3 M NaCl since they are the same conditions in the protein extract (adsorption condition). Cruciferin experiments were performed in duplicate.

As the absolute cruciferin liquid concentration values could not be measured, cruciferin adsorption capacity was determined by dividing Eq. (1) by the reference concentration (C_0) (Eq. (3)), assuming that $\frac{C_{p,eq}}{C_0} = \frac{Area\ at\ equilibirum}{Area\ of\ reference}$

$$\bar{q}_{p,eq} = \frac{q_{p,eq}}{C_0} = \frac{C_{p,load} * V_{load} - C_{p,eq}(V_H + V_{load})}{V_{resin} C_0} \quad (3)$$

The reference cruciferin area peaks were the ones corresponding to the conditions of 0.3 M NaCl and Napin concentration of around 6 g/L for experiments at pH6 (feed condition).

2.5.2. Parameter estimation

Adsorption isotherm experimental results of napin were fitted to a linear isotherm or to a Langmuir type isotherm (Eq. (4)). This to identify the initial isotherm slope, which is an indication of the affinity of napin to the resin.

$$q_{p,eq} = \frac{b_{p,i} q_{p,i}^{max} C_{p,i}}{1 + b_{p,i} C_{p,i}} \quad (4)$$

where $q_{p,i}^{max}$ is the maximum adsorption capacity (mg/mL$_{resin}$) and $b_{p,i}$ is the Langmuir constant also known as equilibrium constant (Carta and Jungbauer, 2010). The initial isotherm slope, at the evaluated conditions, was used to evaluate resin selection (see 2.6 Resin selection).

The most suitable resin equilibrium data (POROS 50 HS) was fitted to the mixed mode isotherm, developed by Nfor et al. (2010). This isotherms is based on the thermodynamic framework of Mollerup et al. (2008). A more detail explanation of this isotherm is found in section 2.8.1 Mixed mode isotherm model of this paper. The fitted parameters of this isotherm model were: 1) the thermodynamic equilibrium constant (K_{eq}); 2) the stoichiometric coefficient of salt counter ion (ν); 3) the parameter that describes the difference between water-protein and protein–protein interactions (K_p) and 4) the parameter that describes the difference between water – protein and salt – protein interactions (K_s). As previously mentioned, binary component experiments (napin + cruciferin) were performed using a protein mixture powder. Binary component adsorption experiments showed a higher napin adsorption capacity than napin single component experiments. For isotherm modelling this was adjusted by considering the value obtained from binary mixture experimental results, which corresponds to 44 mg/mL.

Data regressions were done using MATLAB R2017b and the function *lsqcurvefit*. In the mixed mode model, q_p appears in both sides of the equation (Eq. (7)) The numerical solution of this equation was found using the *fsolve* function of MATLAB and it was combined with the regression using *lsqcurvefit* optimizer. Thus, the procedure of the parameter regression is applying *lsqcurvefit* optimizer to minimize the sum of squared residuals between the experimental data and the numerically solved adsorption data using *fsolve* function.

In addition, as binary mixture experiment presented a very low change in cruciferin concentration. A linear isotherm model was considered for this protein by estimating isotherm slope by fitting a linear curve to the experimental data.

2.6. Resin selection

The generated equilibrium data was used to select the most suitable resin for the separation of both proteins. The desired scenario is the adsorption of napin while cruciferin flows through. The selection criteria were defined as suggested by Sevillano et al. (2014), considering napin adsorption capacity at feed conditions (pH 6 and 0.3 M NaCl) and napin desorption, which was evaluated using the inverse of the lowest isotherm slope determined at the evaluated conditions. The third criterion, selectivity, was evaluated using the ratio between napin and cruciferin isotherm slopes at adsorption conditions. The fourth criterion was the price of the resin obtained from the different suppliers. A weight between 0 and 1 was given to each criterion, being 0.5 for napin capacity, 0.3 for napin desorption, 0.1 for selectivity and 0.1 for price. The reason for giving a low weight to the selectivity criterion had to do with the observed poor binding of cruciferin onto most of the evaluated resins.

Each criterion was normalized and resin score was calculated using Eq. (5).

$$Resin\ score = \sum weight * \frac{criterion}{maximum\ value\ of\ criterion} \quad (5)$$

2.7. Column adsorption/desorption experiments

The highest scoring resin, POROS 50 HS, was used to perform pulse column experiments using napin and the protein mixture (napin + cruciferin). The experiments were performed in an AKTA^{TM}Avant system (GE Healthcare Bio-Sciences AB, Uppsala, Sweden) at room temperature (25 °C) operated with Unicorn 7.0 software. Conductivity, pH and UV at 280 nm signals were monitored during the experiments.

A ValiChrom 11.3–100 POROS® 50 HS (Repligen, Sweden) column was used. The column internal diameter was 1.12 cm

and the total bed height was 10 cm, providing a total column volume of 9.8 mL. Extraparticle and total porosities were determined by pulse injections of blue dextran and 1 M NaCl respectively. The obtained values were 0.83 total porosity (ε_T) and 0.3 for extraparticle porosity (ε_b).

For napin and protein mixture experiments, the column was equilibrated with 50 mM bis-tris pH6 with 0.3 M NaCl buffer for 5 column volumes (CV) at 2.5 mL/min. Then 1 mL of napin solution at 6 g/L was injected in the column (10.1 % CV), column was washed with the equilibration buffer for 5 CV in order to remove non-binding substrates out of the column. Step elution was done by applying 5 CV of elution buffer, Tris-HCl pH 8 with 0.7 M NaCl. After each experiment, the column was regenerated with 1 M NaCl solution for 5 CV as recommended by supplier.

For rapeseed protein mixture, 12 g/L of protein mixture was dissolved in 50 mM Bis-Tris pH 6 with 0.3 M NaCl buffer. This corresponds to 6.84 g/L of napin and 5.16 g/L of cruciferin. The protein mixture solution was then sonicated for 30 min in order to increase protein solubility. The solution was filtered with 0.22 μm PVDF filter before injection in column. After use, the column was stored in 20 % (v/v) ethanol as suggested by supplier.

2.8. Chromatography modeling

2.8.1. Mixed mode isotherm model

The mixed mode adsorption isotherm model from Nfor et al. (2010) was applied in this work. The model is a combination of HIC and IEX models from Mollerup (2007). This mixed mode isotherm is based on the assumption that a protein (P) binds to n amount of ligand (L) by hydrophobic interaction and concurrently exchanges with υ amount of salt counter-ion (S) generating a protein-ligand complex ($L_{n+\upsilon}$) in a fixed stoichiometry as shown in Eq. (6). The stoichiometric coefficient of salt counter ion is defined as the ratio between the protein binding charge divided by the charge of the salt counter ion $\left(\upsilon = \frac{z_p}{z_s}\right)$. In this work, sodium chloride was used as a salt counter ion. The single component adsorption isotherm, based on reaction in Eq. (6), results in the isotherm model described in Eq. (7).

$$P + \upsilon SL + nL \leftrightarrow PL_{n+\upsilon} + \upsilon S \tag{6}$$

$$\frac{q_p}{c_p} = A * \left(1 - \frac{q_p}{q_p^{max}}\right)^{\upsilon+n} * \tilde{\gamma}_p \tag{7}$$

$$\text{where } A = \tilde{K_{eq}}(\Lambda)^{\upsilon+n}\left(\frac{1}{z_s c_s}\right)^{\upsilon}\left(\frac{1}{c}\right)^{n} \text{ and } \tilde{\gamma}_p = exp\left(K_p c_p + K_s c_s\right) \tag{8}$$

In Eq. (7), q_p is the adsorbed protein concentration (mg/mL_{resin}), c_p is the protein concentration in solution (mg/mL), K_{eq} is thermodynamic equilibrium constant of reaction (mL/mg), c_s is the concentration of salt in liquid phase. c is molarity of the solution (assumed to be water concentration (Mollerup, 2007)) and q_p^{max} is maximum adsorption capacity of protein (mg/mL_{resin}), Λ is ligand density of the mixed mode resins which are assumed to be equal for HIC and IEX ligands (mmol/L) and was obtained based on supplier specifications. The activity coefficient of the protein ($\tilde{\gamma}_p$) was determined using the Van der Waals equation of state shown in Eq. (8) as suggested by Mollerup (2006). K_p parameter describes the difference between water-protein and protein–protein interactions while K_s parameter describes the difference between water – protein and salt – protein interactions (Nfor et al., 2010). In the model, $\left(1 - \frac{q_p}{q_p^{max}}\right)$ describes the fraction of free ligands, which is 1 if no protein is bound and decreases asymptotically to zero. This isotherm incorporates the effect of salt concentration in the term C_s.

The mixed mode isotherm described in Eq. (7) reduces to the HIC and IEX isotherm models derived by Mollerup (2006) when $\upsilon = 0$ (electrostatic interactions not present) and $n = 0$ (no hydrophobic interactions), respectively.

2.8.2. Column chromatography model

Column chromatography was simulated based on the transport-dispersive column model which can be described per component as shown in Eq. (9)

$$\frac{\partial c_{p,i}}{\partial t} + \left(\frac{1-\varepsilon_b}{\varepsilon_b}\right)\frac{\partial q_{p,i}}{\partial t} = -\upsilon\frac{\partial c_{p,i}}{\partial x} + D_{L,i}\frac{\partial^2 c_{p,i}}{\partial x^2} \tag{9}$$

where, ε_b is the bed porosity, υ is the interstitial velocity of the mobile phase (m/s), and D_L is the axial dispersion coefficient (m^2/s)

Mass transfer can be quantified by the liquid-film linear driving force approximation. The solid stationary phase concentration term $\frac{\partial q_{p,i}}{\partial t}$ is defined as follows in Eq. (10):

$$\frac{\partial q_{p,i}}{\partial t} = k_{ov,i}\left(C_{p,i} - C^*_{p,eq,i}\right) \tag{10}$$

$k_{ov,i}$ is the overall mas tranfers coefficient (1/s) and $C^*_{p,eq}$.is the bulk equilibrium concentration which is obtained using the mixed mode isotherm (Eq. (7)). Mixed mode isotherm parameters were used to model napin chromatography while a linear isotherm was considered to model cruciferin chromatography.

The film mass transfer coefficient is defined in Eq. (11) (Felinger and Guiochon, 2004).

$$\frac{1}{k_{ov,i}} = \frac{d_p}{6 * k_f} + \frac{d_p^2}{60 * \varepsilon_p * D_p} \tag{11}$$

where d_p is the particle diameter (m), k_f is the film mass transfer coefficient (m/s), ε_p is the intraparticle porosity and D_p is the pore diffusivity (m^2/s). To determine additional relevant model parameters, correlations presented in Table 2 were used.

Column boundary conditions are described by Danckwerts for dispersive systems and it is assumed that the column is not preloaded with the proteins C_p(t=0)=0 and q_p(t=0)=0.

$$C(t, x = 0) = C_{inlet} - \frac{D_L}{u_h}\cdot\frac{\partial C(t, x = 0)}{\partial x} \tag{12}$$

$$\frac{\partial C(t, x = L)}{\partial x} = 0 \tag{13}$$

where x is the axial position. Eq. (12) represents the boundary at the inlet of the column and Eq. (13) the boundary condition at the column outlet. As pulse experiments were performed, the injection profile is modelled as a rectangular pulse with a constant feed concentration for a given time, where $t_{pulse} = V_{inj}/\Phi_v$, where Φ_v is the volumetric flow rate (m^3/s) and V_{inj} is the injection volume.

$$\text{Pulse} \quad C_{inlet}(t) = C_{feed}, i \;\; at \;\; 0 < t < t_{pulse} \tag{14}$$

$$\text{Elution} \quad C_{inlet}(t) = 0 \; at \; t > t_{pulse} \tag{15}$$

Table 2 – Engineering correlations for column modelling.

Mass transfer parameter	Correlation	Reference
Hydrodynamic radius	Stokes Einstein	LeVan et al. (1999)
Free diffusivity	Young	Young et al. (1980)
Film mass transfer coefficient	Wilson & Geankoplis	Wilson and Geankoplis (1966)
Pore tortuosity	Wakao & Smith	Wakao and Smith (1962)
Pore diffusivity	Brenner & Gaydos	Brenner and Gaydos (1977)
Axial dispersion coefficient	Gunn	Gunn (1987)
Pressure drop	Karman-Cozeny	Carta and Jungbauer (2010)

Eq. (9) is a partial differential equation, dependent on time and column position, that can be approximated to an ordinary differential equation by spatial discretization. The method of lines was used to discretize Eq. (9) in space. The set of ordinary differential equations was solved in MATLAB R2017b using the ODE solver *ode15s*.

3. Results and discussion

3.1. *Resin and proteins characteristics*

The used protein isolates, cruciferin, napin and protein mixture were analyzed by SDS-PAGE (Supplementary material). Napin and the protein mixture showed expected band profiles that were comparable to the ones reported elsewhere (Perera et al., 2016). Cruciferin did not shown the expected profile and the solubility of this protein isolate in any of the tested conditions was very limited, therefore the protein mixture was used to evaluate cruciferin isotherms.

To avoid an overestimation of the adsorbed phase protein concentration, the resin liquid hold-up was evaluated. The obtained values were 9.3 μL, 8.7 μL, 7.0 μL, 9.2 μL, 10.0 μL, 9.8 μL, 12.4 μL and 8.5 μL for CaptoMMC, Nuvia cPrime, Toyopearl MX, PPA HyperCel, CaptoS, POROS 50 HS, CM Sepharose and MacroPrep50 CM respectively. These hold up volumes correspond to ~3–4% of the total volume applied in the adsorption experiments (350 μL).

3.2. *Napin adsorption equilibrium isotherms*

Napin adsorption equilibrium isotherms were determined for all resins at feed conditions, (0.3 M NaCl at pH6). Results are shown in Fig. 1, where the experimental napin adsorption capacity is plotted against the equilibrium bulk concentration. From the figure, one can observe that at feed conditions, the highest adsorption capacity is obtained using resin Capto MMC, followed by Nuvia cPrime, POROS HS, PPA HyperCel, Toyopearl, Capto S, MacroPrep and CM Sepharose. Most of the resins showed a maximum limit in the amount adsorbed, which can be described with a Langmuir isotherm model (Eq. (4)). Resins CaptoS and CM Sepharose presented a linear behavior. The experimental data was fitted with two isotherm models - Langmuir or linear type.

In addition to the resin isotherm shape presented in Fig. 1, the affinity of napin to the resins was also obtained by determining the initial isotherm slopes. The initial isotherm slope is an indication of the interaction strength between the protein and the resin. The larger the isotherm slope, the stronger the interaction. At feed conditions, the isotherms' initial slopes, for each resin, can be ranked from largest to smallest: CaptoMMC, Nuvia cPrime, POROS HS, PPA HyperCel, Toyopearl, Macro Prep, Capto S and CM Sepharose. Absolute values (obtained from fitting) can be found in Table 3.

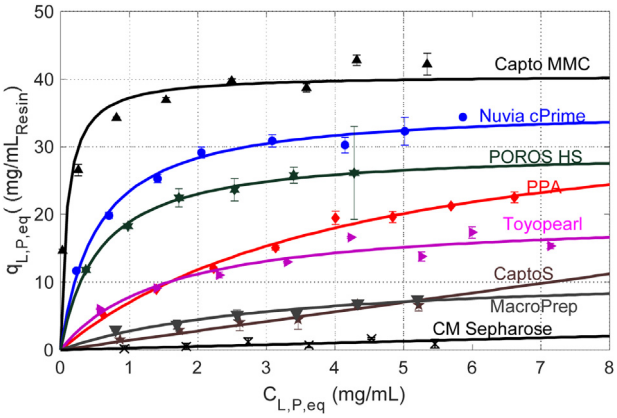

Fig. 1 – Napin adsorption isotherms on mixed mode and ion exchange resins at pH6 and 0.3 M NaCl. Symbols represent experimental results. Error bars resulted from duplicate experiments. Lines represent Langmuir isotherm for CaptoMMC, Nuvia cPrime, POROS HS, Toyopearl, PPA Hypercel and MacroPrep and linear isotherm for Capto S and CM Sepharose.

The difference between the napin binding strength onto the different resins can be explained based on the pKa of the resins (Table 1), the isoelectric point of napin protein - in this case around 11 - and the protein net charge at the evaluated conditions. At pH 6, all resins are negatively charged and napin has a positive net charge. Therefore, attractive electrostatic interactions are possible. However, there is also salt presented in the medium (NaCl) which could promote hydrophobic interactions between napin and the mixed mode resins. A salt concentration of 0.3 M NaCl – which can be considered medium -, proved to be already too high for the weak ion exchangers here evaluated (CM Sepharose and Macro-Perp) and even for the strong cation exchanger Capto S. As the preferable scenario is the adsorption of napin at pH 6 and 0.3 M NaCl, CM Sepharose, Macro-Prep and CaptoS resins were discarded as suitable candidates due to the poor binding of napin under such conditions.

The effect of ionic strength and pH was evaluated for all resins in order to determine suitable desorption conditions.

3.2.1. *Effect of pH on napin adsorption*

The ionic strength and pH might have a significant impact on the adsorption of napin on mixed mode cationic resins, cation exchange resins and the anion mixed mode resin here evaluated. Experiments were performed at different pH values keeping the salt concentration constant at 0.3 M NaCl, which correspond to the same ionic strength as in the protein extract. Napin isotherm results are shown in Fig. 2 and Fig. 3.

From Fig. 2, one can notice that for Capto MMC, Nuvia cPrime and Toyopearl, there is a decrease on napin adsorption

Table 3 – Napin isotherm slope on mixed mode resin and ion exchange resin at pH6 and pH8 and different NaCl (C_s) concentration.

Resin	pH	C_S (M)	Isotherm slope (mL/mL_{resin})	Resin	pH	C_S (M)	Isotherm slope (mL/mL_{resin})
Capto MMC	6	0.1	1185.4 + 245.2	Capto S	6	0.1	146.1 + 12
		0.3	**437.6 + 266.1**			**0.3**	**1.4 + 0.1**
		1.0	23.1 + 7.9			0.7	Not adsorbed
	8	0.1	1114.4 + 248.8		8	0.1	25.2 + 3.8
		0.3	99.3 + 25.6			0.3	0.2 + 0.0
		0.7	17.8 + 6.8			0.7	Not adsorbed
Nuvia cPrime	6	0.1	620.9 + 78.3	POROS 50 HS	6	0.1	453.8 + 76.2
		0.3	**67.5 + 17.23**			**0.3**	**52.5 + 14.9**
		1.0	1.3 + 0.01			0.7	0.7 + 0.9
	8	0.1	276.6 + 57.5		8	0.1	108.9 + 22.5
		0.3	20.2 + 3.5			0.3	6.0 + 1.8
		0.7	2.1 + 0.2			0.7	Not adsorbed
Toyopearl	6	0.1	97.4 + 13.6	CM Sepharose	6	0.1	8.5 + 3.0
		0.3	**5.9 + 5.02**			**0.3**	**0.3 + 0.0**
		1.0	0.4 + 0.2			0.7	Not adsorbed
	8	0.1	52.4 + 9.1		8	0.1	13.5 + 1.9
		0.3	1.8 + 0.3			0.3	0.2 + 0.0
		0.7	0.5 + 0.1			0.7	Not adsorbed
PPA HyperCel	6	0.1	1.9 + 0.1	Macro Prep	6	0.1	67.4 + 14.8
		0.3	**8.5 + 3.4**			**0.3**	**3.6 + 1.3**
		1.0	13.0 + 3.7			0.7	Not adsorbed
	8	0.1	7.7 + 7.5		8	0.1	19.8 + 2.6
		0.3	15.4 + 2.8			0.3	0.8 + 0.1
		0.7	35.4 + 7.9			0.7	Not adsorbed

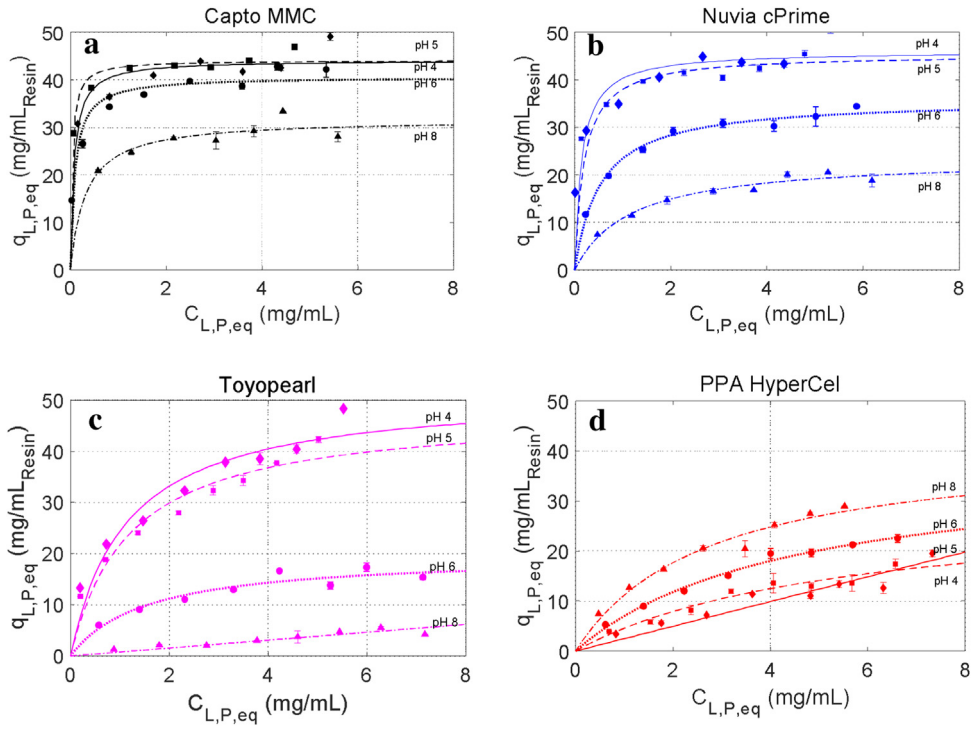

Fig. 2 – Napin adsorption isotherms at different pH keeping salt concentration at 0.3 M NaCl a) Capto MMC resin, b) Nuvia cPrime resin, c) Toyopearl resin and d) PPA HyperCel resin. Symbols represent experimental results. Error bars resulted from duplicate experiments. Lines represent the Langmuir isotherm.

capacity with increasing pH. This can be explained by the protein's net charge and the resin ligand's pKa. The weak cation exchangers are negatively charged at pH higher than the pKa, while the opposite occurs for weak anion exchangers, which are positively charged at pH lower than the pKa. Strong cation exchangers are practically always charged at any pH (Carta and Jungbauer, 2010). The interactions between mixed mode resins and proteins have been explained by different authors (Nfor et al., 2010). The interaction is strongest close to the pKa of the ligand and decreases if the pH is close to the pI of the protein, which is clearly observed here for Toyopearl, Capto MMC, Nuvia cPrime and POROS HS. At pH 4, the net charge of napin is around 12 while at pH 8, the net charge decreases significantly to around 4. The net charge of napin at different pH values was estimated using the using the amino acid

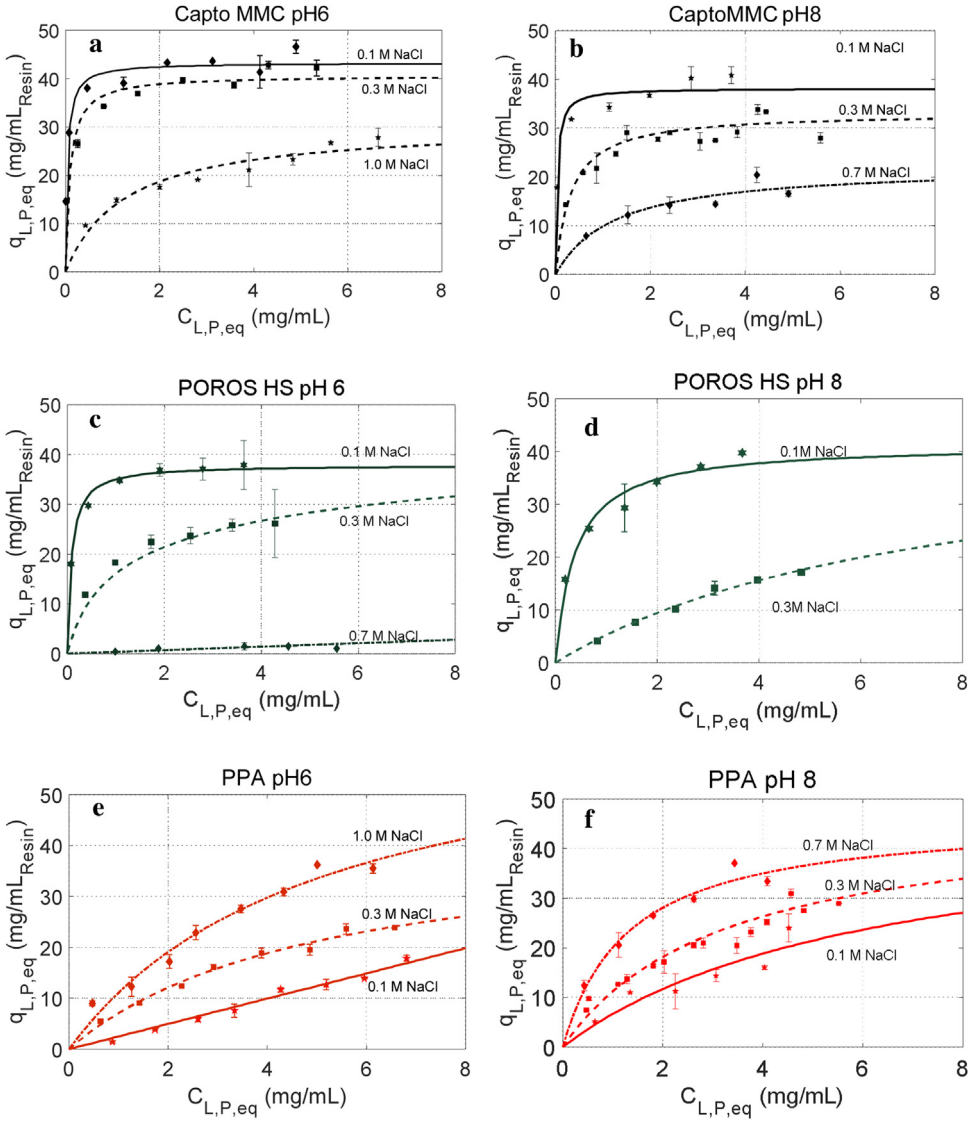

Fig. 3 – Effect of ionic strength on napin adsorption on Capto MMC, POROS HS and PPA HyperCel at pH6 and pH8. Symbols represent experimental results. Error bars resulted from duplicate experiments. Lines represent the mixed mode isotherm that the data has been fitted to.

sequence (obtained from the RCSB Protein Data Bank (PBD)) and Eq. (16) (Supplementary materials).

$$z_{net} = \sum_{i} \frac{N_{basic,i}}{1+10^{pH-pKa_i}} - \frac{N_{acidic,i}}{1+10^{pH-pKa_i}} \quad (16)$$

Where z_{net} is the net charge $N_{basic,i}$ is the number of basic amino acids and N terminal, and $N_{acidic,i}$ is the number of basic amino acids and C terminal.

The opposite behavior is observed with the weak anion mixed mode resin PPA HyperCel: an increase in adsorption capacity with an increase of pH. Since the pKa of the PPA HyperCel resin ligand is around 8, the resin is positively charged. Because napin is also positively charged at all the evaluated pH values, there is an electrostatic repulsion between the resin and the protein. The adsorption is consequently a result of the hydrophobic interactions between napin and the resin and the electrostatic repulsion. The pH has a big influence on the adsorption of napin in PPA resin, as the isotherm slope and isotherm shape change with pH: there is a higher napin affinity to the resin at a higher pH. However, the adsorption capacity is still lower than the maximum obtained at feed condition pH 6 and 0.3 M NaCl with other resins (e.g. 40 mg/mL by Capto MMC), which decreases PPA resin score.

Even though, there is a notorious change on napin adsorption at different pH values, the Capto MMC resin is the least influenced, showing a favorable isotherm even at pH 8. On the other hand, napin adsorption strength on Nuvia cPrime, POROS 50 HS and Toyopearl is significantly reduced. The isotherm slopes of all the resins at different conditions are indicated in Table 3.

The isotherm slope represents the affinity of the protein to the resin (the binding strength) which is clearly much higher for Capto MMC at almost any pH value. However, this is not necessary an advantage, as a higher pH might be needed to desorb napin with this resin, possibly interfering with its native structure, stable between pH 3–12 (Wanasundara, 2011), thus with its physico-chemical properties.

These results can be used to identify desorption conditions of the best performing resin.

3.2.2. *Effect of ionic strength on napin adsorption*

Higher ionic strength is known to promote hydrophobic interactions due to the so-called "salting-out" effect. Three different salt concentrations (ionic strengths) were tested at two different pH conditions. Most of the tested resins showed similar trends: a decrease of napin adsorption strength with an increase of ionic strength. This can be observed by the lower isotherm slope values and experimental capacities obtained at higher salt concentrations (See Fig. 3 and Table 3). This suggests that napin adsorption on mixed mode resins is mainly controlled by ionic interactions.

The exception was PPA resin, which presented an increase in napin adsorption with increasing salt concentration. As previously mentioned, since for this resin electrostatic interactions are repulsive, an increase in the binding capacity of napin should be mainly due to an increase in the strength of hydrophobic interactions. No significant improvement in the adsorption of napin was observed between pH 6 and pH 8, at different salt concentrations. This might support the fact that napin adsorption on PPA HyperCel is characterized only by hydrophobic interactions in that range.

Based on the isotherm slope, one can notice that Capto MMC has the largest affinity for napin. However, this might complicate the desorption and recovery of the protein after the capture step, as even at high pH and salt concentrations the isotherm is favorable. As a consequence, especially harsh conditions (e.g. pH higher than the pI of the napin) might need to be applied. The determined napin isotherm slopes at all tested conditions are shown in Table 3.

From the obtained results it is clear that the effect of ionic strength is more significant than the effect of pH, especially for the PPA HyperCel resin. When comparing the results for that resin (Fig. 3e and f), the isotherms seem to overlap. This was expected, as the adsorption of napin occurs mainly through hydrophobic interactions. This effect can be evaluated by comparing the ratio between the isotherm slopes at two different salt concentration (at a specific pH) and the ratio between the isotherm slopes at two different pH conditions (at a specific salt concentration).

Similar isotherm trends to the ones determined in this work were observed in the research of Nfor et al. (2010). The authors evaluated lysozyme (similar pI and molecular weight as napin) adsorption on Capto MMC and PPA HyperCel. The adsorption capacity of lysozyme was in the same order of magnitude as the one obtained for napin in this work. In addition, similar isotherm curves were observed when comparing two pH values and one salt concentration.

All this information was used to select the most suitable resin for napin capture.

3.3. *Protein mixture adsorption experiments*

Batch adsorption experiments were performed using solutions of a protein mixture (napin + cruciferin), to evaluate both, the effect of cruciferin on napin's adsorption and to determine cruciferin's adsorption isotherms. At feed conditions, it is expected that cruciferin poorly binds to the resins, as the pH is close to the pI of this protein (~7). A comparison between the expected napin adsorption capacity and the adsorption capacity obtained from the experiments using the protein mixture was done and the results can be found in Fig. 4.

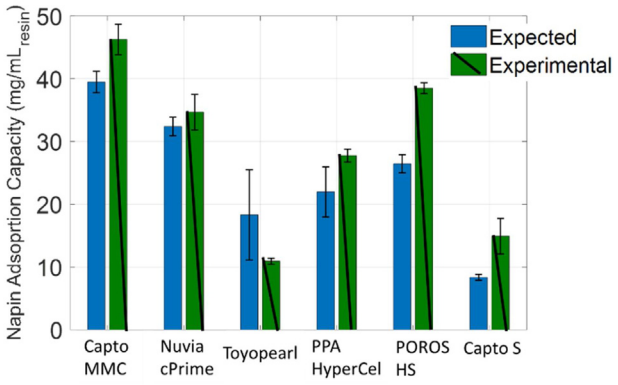

Fig. 4 – Napin adsorption capacity comparison between expected capacity and experimentally obtained from protein mixture experiments at pH6 and 0.3 M NaCl. Expected capacity was calculated from single component isotherm.

The presence of cruciferin seems to enhance napin adsorption at pH6 and 0.3 M NaCl for POROS HS and CaptoS where higher adsorption capacities than expected were obtained. This behavior might be explained by the charge of the proteins. At pH 6, both cruciferin and napin possess a positive net charge, allowing cruciferin to bind to the resins as well. However, cruciferin is considered a large protein, and in solution with napin, the positive charge on cruciferin's surface might have resulted in a strong electrostatic repulsion of napin molecules. By creating a less favorable chemical environment in the liquid solution, the presence of cruciferin might then be improving the adsorption of napin molecules onto the tested resins.

In all experiments (Supplementary material), cruciferin showed a very small change in concentration after equilibration with the resins, which indicated a low binding strength. Only resin PPA HyperCel showed a relatively high cruciferin concentration change. The cruciferin's isotherm slope values were obtained by fitting a linear curve to the experimentally obtained capacities (as function of the equilibrium liquid concentrations). The obtained values were 2.0 + 1.3, 0.8 + 0.1, 2.3 + 1, 22.1 + 8.2, 1.6 + 0.5 and 0.9 + 0.7 mL/mL$_{resin}$ for Capto MMC, Nuvia cPrime, Toyopearl, PPA HyperCel, POROS HS and Capto S respectively. Cruciferin's isotherm slope is significantly lower than the one of napin for resin Capto MMC, Nuvia cPrime and POROS HS, suggesting a preferential binding of napin to these resins. Napin isotherm slope values were slightly higher for resins CaptoS and Toyopearl and cruciferin's isotherm slope was higher than napin's isotherm slope for resin PPA HyperCel. As discussed before, for PPA HyperCel resin, binding is mainly characterized by hydrophobic interactions. Because, cruciferin is a more hydrophobic molecule than napin, this might explain the higher affinity towards this resin. All the obtained results were used to identify the most suitable resin for the capture of napin.

3.4. *Resin selection*

The most suitable resin for the separation of napin an cruciferin was selected using the previously defined selection criteria (2.6 Resin selection). 1) Napin adsorption capacity at feed conditions (pH6 with 0.3 M NaCl), 2) best desorption conditions (based on the lowest isotherm slope obtained for each resin), 3) selectivity of napin over cruciferin and 4) resin

Table 4 – Values of each criterion (napin capacity, selectivity, resin price and desorption) used for resin selection and resin scores.

	Napin capacity[a] (mg/mL)	Selectivity[b] (-)	1/slope desorption[c] (mL_{resin}/mL)	Price/highest price (-)	Resin score
Capto MMC	**40.0**	**219.9**	0.1[d]	0.8	66%
Nuvia cPrime	34.3	81.3	0.8[e]	0.8	57%
Toyopearl	14.1	2.5	2.6[f]	1.0	37%
PPA HyperCel	26.6	0.4	0.5[g]	1.0	41%
POROS HS50	30.0	33.0	**5.6**[h]	**0.5**	75%

[a] Napin capacity at 0.3 M NaCl and pH 6.
[b] Ratio between napin an crucferin isotherm slopes at 0.3 M NaCl and pH 6.
[c] Inverse of isotherm slope:
[d] at 0.7 M NaCl and pH 8;
[e] at 1.0 M NaCl and pH 6;
[f] at 1.0 M NaCl and pH 6;
[g] at 0.1 M NaCl and pH 6;
[h] at 0.7 M NaCl and pH 8.

price. Adsorption (napin capacity) and desorption were the two criteria with higher importance in the selection process. As previously mentioned, resins CaptoS, CM Sheparose and MacroPrep where discarded, as they showed significantly lower napin capacity compared to the other resins at feed conditions. The results are shown in Table 4.

Even though resin Capto MMC possesses the highest napin capacity (in all conditions tested) and selectivity, this resin was not selected as the most promising. The reason has to do mainly with desorption, possibly requiring a pH higher than napin's pI, which, as previously mentioned, can lead to problems with the structural stability of napin. Therefore, desorbing at a pH above the pI is not recommended. The best performing resin in terms of desorption performance was POROS HS, since its results indicate that desorption can be performed at high salt concentration without increasing the pH to a higher value than napin's pI. Despite being second best on desorption criteria. the Toyopearl resin also showed a much lower adsorption capacity for napin when compared to Capto MMC and Nuvia cPrime at feed conditions. Therefore, the Toyopearl resin scored the lowest in the adsorption capacity criterion.

PPA HyperCel and POROS HS showed comparable adsorption capacities at feed condition. Nevertheless, from the experiments performed with the protein mixture it was clear that cruciferin also interacts with resin PPA HyperCel having an even larger isotherm slope than napin. This was observed with the obtained selectivity value which was lower than unity, indicating that at pH6 and 0.3 M NaCl, cruciferin interacts more favorably with PPA HyperCel resin than napin.

The last evaluated selection criterion was resin cost, with resin POROS HS being the cheapest one, as the price range is around half the price obtained for the mixed mode resins. Even though this criterion was evaluated with a lower weight, it was taken into account, as process economics is a significant factor in process development.

3.5. *Mixed mode isotherm parameter estimation*

Napin adsorption data obtained for POROS HS resin was used in order to fit the isotherm model described in 2.8.1 Mixed mode isotherm model. Since POROS HS is a strong cation resin, there are no hydrophobic interactions presented and the parameter n from Eq. (7) was set to zero. In order to reduce the complexity of solving the non-linear system, the model was linearized by applying the natural logarithm in both sides of the equation and the regression was performed as explained in 2.5.2 Parameter estimation. The experimental data from the three evaluated salt concentrations were fitted to determine the set of parameters K_{eq}, υ, K_p and K_s, for each pH value. The maximum adsorption capacity (q_p^{max}) was obtained from adsorption equilibrium experiments from protein mixture and the obtained value was 44 mg/mL_{resin}. The regressed parameters are shown in Table 5.

The stoichiometric coefficient (υ) of the salt counter ion at pH6 was higher than at pH8, which was expected. For this system, υ is equal to protein binding charge. At pH values approaching the pI of the protein (napin pI ~11), the net charge of the protein approaches zero (lower) and the electrostatic binding strength becomes weaker, resulting in a lower binding capacity. K_p is the parameter that describes the difference between water-protein and protein–protein interactions (Mollerup, 2006). The regressed K_p for both pH values (6 and 8) had a positive value, suggesting that interactions between protein-water were stronger than protein-protein interactions. This also matches the observations obtained in this work and the data from literature, indicating a high solubility of napin in water. Similar to K_p, the parameter K_s describes the difference between water–protein and salt–protein interactions (Mollerup, 2006). The obtained K_s values at both evaluated pH conditions were around zero, implying that the strength of protein-salt interactions is not significantly different than protein-water interactions. By analyzing the two different interaction parameters - K_p and K_s -, the strength of water-protein, protein-salt and protein-protein interactions could be inferred. In this system, given that K_p >0 and K_s ≈0, protein-water interactions were dominant.

The pH value of mobile phase has an influence on the binding charge of the protein which consequently changes the υ value and it is expected to be lower when the pH is closer to the pI of the protein. In order to include the influence of pH on the stoichiometric coefficient, approaches like the one from Pirrung et al. (2018) could be used. The υ for POROS decreases with increasing of pH which corresponds to the influence of pH on electrostatic interactions.

A linear isotherm model was considered for cruciferin protein due to the low binding observed with resin POROS HS.

Table 5 – Ion exchange isotherm parameters of napin protein in POROS HS resin at pH6 and pH8.

	ln K_{eq}	v	K_P (mM^{-1})	K_S (mM^{-1})	R^2	SD
POROS HS pH6	6.6 + 0.3	1.9 ± 0.4	2.3 ± 2.7	$-5 \times 10^{-3} + 1 \times 10^{-3}$	0.97	0.2
POROS HS pH8	5.8 ± 0.2	1.2 ± 0.2	0.8 ± 1.0	$-9 \times 10^{-3} + 8x10^{-3}$	0.98	0.1

3.6. *Column chromatography*

Two pulse experiments were performed at small scale (~10 mL column volume) using either a solution of napin or a solution of protein mixture (napin + cruciferin). The experimental results were compared with the model output and can be found in Fig. 5. The data obtained from the chromatography station was normalized for easier comparison with the modeling results.

As can be seen in Fig. 5, the model is in excellent agreement with the experimental results for napin as single component and also when napin is in the presence of the second protein, cruciferin. Analyzing napin results (Fig. 5a), one can notice that no desorption of napin occurs after 5 CV of washing step, which suggests a strong binding at these conditions (as shown by the determined isotherm). Elution with high salt concentration (0.7 M NaCl) and pH8 shows a very sharp peak. This was expected as at these conditions, napin capacity in POROS HS is close to zero. High salt and pH conditions were chosen in order to have high recovery, which correspond to 100% based on mass balance (evaluated by numerical integration). Note that high pH might not be needed to fully desorb this protein. After desorption phase, the column was washed with a concentrated salt solution (1 M NaCl) until no absorbance at 280 nm was detected. The maximum napin concentration detected was 6.8 + 0.1 g/L.

Protein mixture chromatogram is presented in Fig. 5b. Napin elution profile using this binary mixture corresponds to the one obtained using single component napin. After applying the elution buffer, again a sharp peak is observed with a peak maximum at around 6.0 CV (approximately one column volume after the switch in conditions). In this experiment, an extra peak is observed during the washing step, which might correspond to cruciferin protein. Using a linear isotherm model for cruciferin protein (slope 1.6 mL/mL) and performing the simulation, one can observed a peak at around 1.8CV (washing step). Comparing cruciferin simulation results with experimental results, it is clear that cruciferin isotherm slope was overestimated. This because the experimental peak exited the column earlier (~1CV) and it is sharper but also presented tailing. This tailing might be caused by the size of cruciferin, which is around 300 kDa. The difference between the experimental and simulated results might be attributed to cruciferin equilibrium parameter. As previously mentioned, during binary mixture experiments cruciferin data presented very small changes which were difficult to quantify. Besides these difficulties, the model shows excellent agreement in respect to napin protein. The maximum napin concentration obtained in the chromatogram of the protein mixture pulse experiment was 7.8 + 0.1 g/L. This value is higher than the one obtained in the experiment with pure napin experiment due to the slightly higher napin concentration applied.

Using column experimental results from the protein mixture, the slope of cruciferin was calculated to be 0.6 mL/mL_{resin}, which consequently increased the selectivity of napin to POROS HS resin to 87.0.

The validated model can be then used for industrial column design to identify column sizing and operating parameters. Scale up of chromatography processes from laboratory results is usually done by keeping bed height and velocity constant and changing column diameter. However, this makes scalability inflexible, often resulting in column volumes that cannot satisfy the desired capacity or that do march the capacities found at pilot and industrial scale, where companies often possess already existing equipment. Pre-determined volumes (Staby et al., 2017), with fixed column diameter and adjustable headers. The use of the previous model could reduce the number of experiments or investment required to satisfy production.

The following section describe the use of the previous model to design an ion exchange column for the separation of these proteins. The model was applied to a hypothesized case study considering the production of rapeseed meal in the Netherlands. This case study can be used as base for large scale purification of oilseed meals.

3.7. *Adsorptive process design for the purification of napin, cruciferin and sinapic acid from rapeseed meal*

Rapeseed production has significantly increased in the last years, having a global production of 75 million Mt in 2018 where 25 million Mt were produced in Europe (Food and Agriculture Organization of the United Nations (FAO), 2019). As mentioned before the main product obtained from rapeseed is oil for human consumption, usually extracted from the seed by mechanical and solvent extraction (Fetzer et al., 2018; Wanasundara et al., 2017). As byproduct, rapeseed meal with a high protein content (~40% dry basis), mainly consisting of cruciferin and napin (Contreras et al., 2019; Lomascolo et al., 2012; Wanasundara et al., 2017) is generated. In the Netherlands, around 3500 MT of rapeseed meal were generated in 2018, corresponding to around 1400 MT of total protein. A conceptual downstream process (DSP) of rapeseed meal for the purification of proteins and polyphenols is shown in Fig. 6. The DSP includes: an aqueous extraction assisted with salts (Bérot et al., 2005) to solubilize the different components in the meal, followed by a small molecule separation (phytic acid, polyphenols compounds, carbohydrates) using ultrafiltration with a cut-off membrane of 3 kDa. The protein rich retentate is sent to an ion exchange (IEX) column where napin is captured and cruciferin flows through. The permeate can be further processed to recover sinapic acid (major polyphenol in rapeseed meal) using adsorption (hydrophobic resins), as recommended by Moreno-González et al. (2020) and Silva et al. (2018a) or liquid-liquid extraction (with organic solvents or ionic liquids) as suggested by Silva et al. (2018b). The purified fractions of napin and cruciferin, obtained after the chromatography column, are then sent to another membrane unit to remove the salts before being sent to the final drying stage. Following the adsorption method for sinapic acid recovery from Moreno-González et al. (2020), elution and regeneration of the adsorption column can be done with ethanol/water mix-

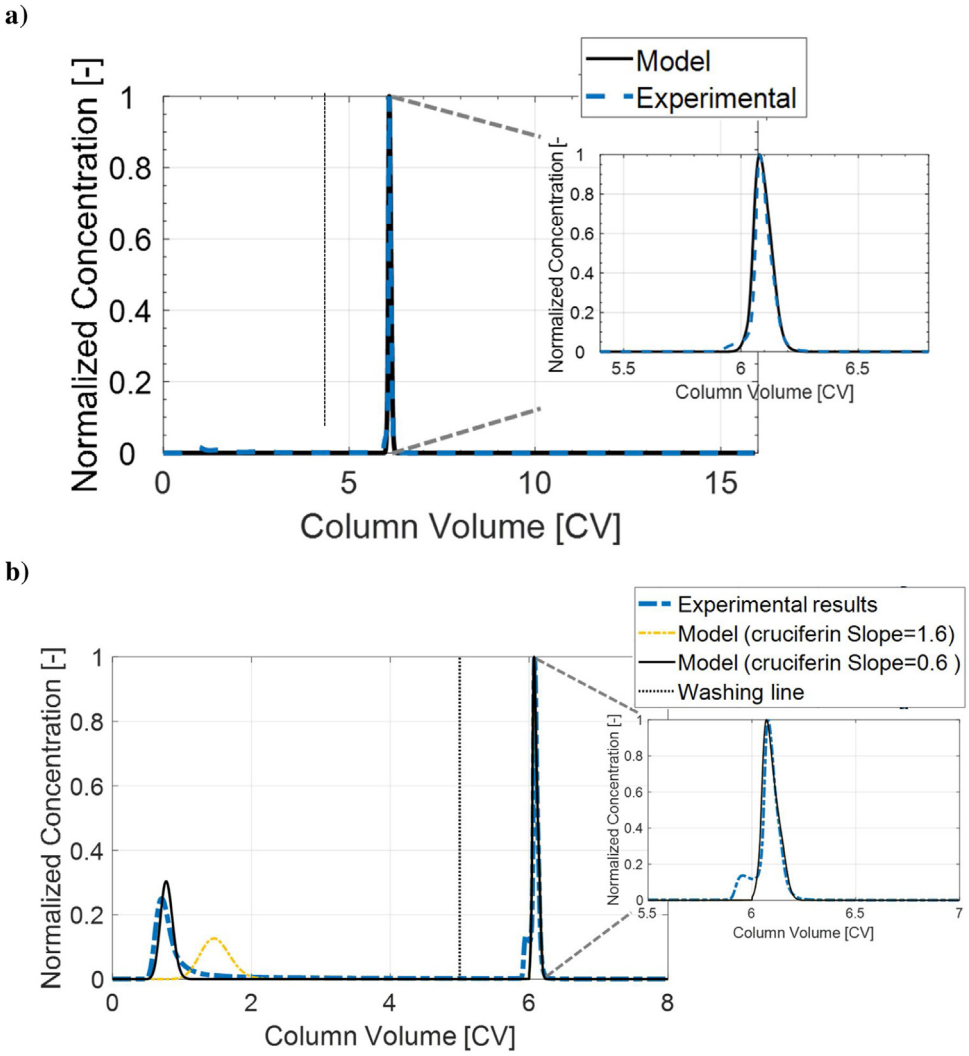

Fig. 5 – Model prediction vs Experimental data of Napin (a) and Protein mixture (b) on POROS 50HS column. Loading condition pH 6 and 0.3 M NaCl, step elution at pH 8 and 0.7 M NaCl. Concentration data was normalized.

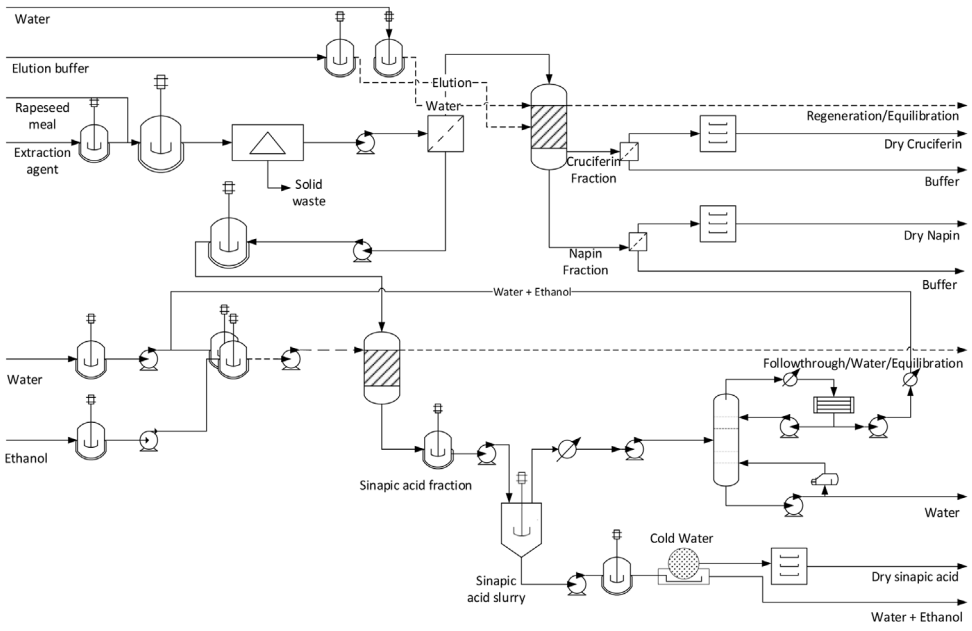

Fig. 6 – Conceptual process design for purification of napin, cruciferin and sinapic acid from rapeseed meal.

tures which can be recovered by distillation and recycled to the column. To obtain sinapic acid crystals, a multiple effect evaporation can be used to crystalize the polyphenol (Silva et al., 2018b). The evaporated solvent is directed to the distillation column and sinapic acid crystals are then filtered, washed and dried.

Considering that the annual production of rapeseed in the Netherlands is 5836 tons (Food and Agriculture Organization of the United Nations (FAO), 2019) and assuming that the first stages of the process (aqueous extraction, centrifugation, small molecules separation) account an overall protein yield of 90% the initial protein extract flow rate can be estimated.

The ion exchange column for protein purification can be sized using the previous model. The selected resin POROS 50 HS has a polymeric matrix (rigid particles) and a particle size of 50 μm and based on supplier specification, this resin possesses high mechanical resistance (100 bars). For a stainless-steel column, a maximum of 50 bar pressure drop was set for a column diameter of 1 m (Schmidt-Traub et al., 2013). Maximum column height using this resin can be estimated using Karman-Cozeny equation, and it corresponds to 1 m.

The column model is then used to determine the operation of the ion exchange column, in specific to identify the loading volume, which is this case is two column volumes. The loading volume is low because the concentration of each protein in the protein rich extract is relatively high (higher than 8 g/L) and the resin gets to equilibrium saturation with relatively low volume. For this simulation, an isotherm slope of 0.6 mL/mL_{resin} was considered for cruciferin equilibrium. The model indicates a resin utilization of 82% and a napin yield of 98% with >99% purity. In the flowthrough, cruciferin is recovered (>99% yield and >98% purity). The productivity calculated with this column size (1 m diameter and 1 m height) is 26.3 $gNapin/L_R/h$, which consequently produces 52.1 MT/a. This accounts to 12% of the total amount of napin than can be recovered from the rapeseed meal generated in the Netherlands using one ion exchange column.

It is possible to purify the annual production of rapeseed meal by calculating the number of columns needed to operate in parallel and the number of cycles that each column can be run. It is important to keep in mind that this is a preliminary evaluation and that breakthrough curve experiments for napin will be still needed to corroborate the selected loading. In addition, for this estimation a similar column operation in terms of desorption was selected (5CV) which could be reduced, as based on the column experiments, full napin recovery might be achieved with less volume. Operation of the ion exchange column can also be adapted to continuous (Simulated moving bed) or semi-continuous (CaptureSMB and Periodic Countercurrent Chromatography, PCC) with multiple columns connected in series or operating in parallel. In addition, economic feasibility should be assessed with a detail economic evaluation to identify overall capital expenditure (CAPEX) and the overall operational cost (OPEX) and performing for instance a cash flow analysis.

4. Conclusions

High throughput process development (HTPD) generates reliable and significant information in a short time period. In the case of adsorptive processes, HTPD, different resins and conditions could be assessed in parallel which allows proper resin choice. The generated information can be used in combination with mechanistic models to evaluate technical feasibility of a process design which involves process understanding and contributes to fast process development.

Declaration of interests

The authors declare that they have no known competing financial interests or personal relationships that could have appeared to influence the work reported in this paper.

Acknowledgments

This work was supported by the ISPT (Institute of Sustainable Process Technology) under the project CM-20-07 in Adsorption of non-volatiles from food products. Thanks to the industrial partners DSM, Unilever, Friesland Campina and Royal Cosun for their valuable input through the project. The authors are also thankful to Yi Song from Delft University of Technology for all the provided lab support.

Appendix A. Supplementary data

Supplementary material related to this article can be found, in the online version, at doi:https://doi.org/10.1016/j.fbp.2020.11.011.

References

Sevillano, D.M., van der Wielen, L.A.M., Hooshyar, N., Ottens, M., 2014. Resin selection for the separation of caffeine from green tea catechins. Food Bioprod. Process. 92, 192–198.

Adachi, M., Kanamori, J., Masuda, T., Yagasaki, K., Kitamura, K., Mikami, B., Utsumi, S., 2003. Crystal structure of soybean 11S globulin: glycinin A3B4 homohexamer. Proc. Natl. Acad. Sci. U.S.A. 100, 7395–7400.

Aider, M., Barbana, C., 2011. Canola proteins: composition, extraction, functional properties, bioactivity, applications as a food ingredient and allergenicity – a practical and critical review. Trends Food Sci. Technol. 22, 21–39.

Akbari, A., Wu, J., 2015. An integrated method of isolating napin and cruciferin from defatted canola meal. LWT - Food Sci. Technol. 64, 308–315.

Bérot, S., Compoint, J.P., Larré, C., Malabat, C., Guéguen, J., 2005. Large scale purification of rapeseed proteins (Brassica napus L.). J. Chromatogr. B. 818, 35–42.

Brenner, H., Gaydos, L.J., 1977. The constrained brownian movement of spherical particles in cylindrical pores of comparable radius: models of the diffusive and convective transport of solute molecules in membranes and porous media. J. Colloid Interface Sci. 58, 312–356.

Carta, G., Jungbauer, A., 2010. Protein Chromatography: Process Development and Scale-up. John Wiley & Sons.

Contreras, Md.M., Lama-Muñoz, A., Manuel Gutiérrez-Pérez, J., Espínola, F., Moya, M., Castro, E., 2019. Protein extraction from agri-food residues for integration in biorefinery: potential techniques and current status. Bioresour. Technol. 280, 459–477.

Felinger, A., Guiochon, G., 2004. Comparison of the kinetic models of linear chromatography. Chromatographia 60 (Suppl. 1), S175–S180.

Fetzer, A., Herfellner, T., Stäbler, A., Menner, M., Eisner, P., 2018. Influence of process conditions during aqueous protein extraction upon yield from pre-pressed and cold-pressed rapeseed press cake. Ind. Crop Prod. 112, 236–246.

Food and Agriculture Organization of the United Nations (FAO), 2019. FAOSTAT Production Quantity (accessed 24 March 2019) http://www.fao.org/faostat/en/#data/QC.

Gerzhova, A., Mondor, M., Benali, M., Aider, M., 2015. A comparative study between the electro-activation technique

and conventional extraction method on the extractability, composition and physicochemical properties of canola protein concentrates and isolates. Food Biosci. 11, 56–71.
Ghodsvali, A., Khodaparast, M.H.H., Vosoughi, M., Diosady, L.L., 2005. Preparation of canola protein materials using membrane technology and evaluation of meals functional properties. Food Res. Int. 38, 223–231.
Gunn, D.J., 1987. Axial and radial dispersion in fixed beds. Chem. Eng. Sci. 42, 363–373.
Hou, F., Ding, W., Qu, W., Oladejo, A.O., Xiong, F., Zhang, W., He, R., Ma, H., 2017. Alkali solution extraction of rice residue protein isolates: influence of alkali concentration on protein functional, structural properties and lysinoalanine formation. Food Chem. 218, 207–215.
Jyothi, T., Sinha, S., Singh, S.A., Surolia, A., Rao, A.A., 2007. Napin from Brassica juncea: thermodynamic and structural analysis of stability. Biochimica et Biophysica Acta (BBA)-Proteins and Proteomics 1774, 907–919.
Kodagoda, L.P., Nakai, S., Powrie, W.D., 1973. Some functional properties of rapeseed protein isolates and concentrates. Canadian Institute of Food Sci. Technol. J 6, 266–269.
LeVan, D.M., Carta, G., Yon, C.M., 1999. Adsorption and ion Exchange. In: Perry, R.H., Green, D.W. (Eds.), Perry'S Chemical Engineers' Handbook. , seven ed. McGraw-Hill, New York, pp. 16–19.
Lomascolo, A., Uzan-Boukhris, E., Sigoillot, J.-C., Fine, F., 2012. Rapeseed and sunflower meal: a review on biotechnology status and challenges. Appl. Microbiol. Biotechnol. 95, 1105–1114.
Mollerup, J.M., 2006. Applied thermodynamics: a new frontier for biotechnology. Fluid Phase Equilibr. 241, 205–215.
Mollerup, J.M., 2007. The thermodynamic principles of ligand binding in chromatography and biology. J. Biotechnol. 132, 187–195.
Mollerup, J.M., Hansen, T.B., Kidal, S., Staby, A., 2008. Quality by design—thermodynamic modelling of chromatographic separation of proteins. J. Chromatogr. A 1177, 200–206.
Moreno-González, M., Girish, V., Keulen, D., Wijngaard, H., Lauteslager, X., Ferreira, G., Ottens, M., 2020. Recovery of sinapic acid from canola/rapeseed meal extracts by adsorption. Food Bioprod. Process. 120, 69–79.
Murray, D.E., Terrence, M.J., Barker, L.D., Myers, C.D., US4208323A, USA patent 1980. Process for Isolation of Proteins Using Food Grade Salt Solutions at Specified pH and Ionic Strength.
National Center for Biotechnology Information, 2020. PubChem Database. Tryptophan, CID=6305 (accessed on Jan. 16, 2020) https://pubchem.ncbi.nlm.nih.gov/compound/Tryptophan.
Nfor, B.K., Noverraz, M., Chilamkurthi, S., Verhaert, P.D., van der Wielen, L.A., Ottens, M., 2010. High-throughput isotherm determination and thermodynamic modeling of protein adsorption on mixed mode adsorbents. J. Chromatogr. A 1217, 6829–6850.
Perera, S.P., McIntosh, T.C., Wanasundara, J.P., 2016. Structural Properties of cruciferin and napin of brassica napus (canola) show distinct responses to changes in ph and temperature. Plants. 5, 36.
Pickardt, C., Neidhart, S., Griesbach, C., Dube, M., Knauf, U., Kammerer, D.R., Carle, R., 2009. Optimisation of mild-acidic protein extraction from defatted sunflower (*Helianthus annuus L.*) meal. Food Hydrocoll. 23, 1966–1973.
Pirrung, S.M., Parruca da Cruz, D., Hanke, A.T., Berends, C., Van Beckhoven, R.F.W.C., Eppink, M.H.M., Ottens, M., 2018. Chromatographic parameter determination for complex biological feedstocks. Biotechnol. Prog. 34, 1006–1018.
Pudel, F., Tressel, R.P., Düring, K., 2015. Production and properties of rapeseed albumin. Lipid Technol. 27, 112–114.
Raab, B., Schwenke, K.D., 1984. Simplified isolation procedure for the 12 S globulin and the albumin fraction from rapeseed (*Brassica napus L.*). Nahrung 28, 863–866, http://dx.doi.org/10.1002/food.19840280820.
Rommi, K., Ercili-Cura, D., Hakala, T.K., Nordlund, E., Poutanen, K., Lantto, R., 2015. Impact of total solid content and extraction ph on enzyme-aided recovery of protein from defatted rapeseed (*Brassica rapa L.*) press cake and physicochemical properties of the protein fractions. J. Agric. Food Chem. 63, 2997–3003.
Schmidt, I., Renard, D., Rondeau, D., Richomme, P., Popineau, Y., Axelos, M.A.-V., 2004. Detailed physicochemical characterization of the 2s storage protein from rapeseed (*Brassica napus L.*). J. Agric. Food Chem. 52, 5995–6001.
Schmidt-Traub, H., Schulte, M., Seidel-Morgenstern, A., 2013. Preparative Chromatography, second ed. John Wiley & Sons, Incorporated, Weinheim, Germany.
Silva, M., Castellanos, L., Ottens, M., 2018a. Capture and purification of polyphenols using functionalized hydrophobic resins. Ind. Eng. Chem. Res. 57, 5359–5369.
Silva, M., García, J.C., Ottens, M., 2018b. Polyphenol liquid-liquid extraction process development using NRTL-SAC. Ind. Eng. Chem. Res. 57, 9210–9221.
Staby, A., Rathore, A.S., Ahuja, S., 2017. Preparative Chromatography for Separation of Proteins. John Wiley & Sons, Incorporated, New York.
Vuorela, S., Meyer, A.S., Heinonen, M., 2004. Impact of isolation method on the antioxidant activity of rapeseed meal phenolics. J. Agric. Food Chem. 52, 8202–8207.
Wakao, N., Smith, J.M., 1962. Diffusion in catalyst pellets. Chem. Eng. Sci. 17, 825–834.
Wanasundara, J.P., 2011. Proteins of Brassicaceae oilseeds and their potential as a plant protein source. Crit. Rev. Food Sci. Nutr. 51, 635–677.
Wanasundara, J.P.D., McIntosh, T.C., Perera, S.P., Withana-Gamage, T.S., Mitra, P., 2016. Canola/rapeseed protein-functionality and nutrition. OCL 23 (4), D407.
Wanasundara, J.P.D., Tan, S., Alashi, A.M., Pudel, F., Blanchard, C., 2017. Chapter 18 - proteins from canola/rapeseed: current status. In: Nadathur, S.R., Wanasundara, J.P.D., Scanlin, L. (Eds.), Sustainable Protein Sources. Academic Press, San Diego, pp. 285–304.
Wilson, E.J., Geankoplis, C.J., 1966. Liquid mass transfer at very low Reynolds numbers in packed beds. Ind. Eng. Chem. Fundam 5 (1), 9–14.
Xu, L., Diosady, L.L., 2002. Removal of phenolic compounds in the production of high-quality canola protein isolates. Food Res. Int. 35, 23–30.
Young, M.E., Carroad, P.A., Bell, R.L., 1980. Estimation of diffusion coefficients of proteins. Biotechnol. Bioeng. 22, 947–955.
Zhang, S.B., Wang, Z., Xu, S.Y., 2007. Downstream processes for aqueous enzymatic extraction of rapeseed oil and protein hydrolysates. J. Am. Oil Chem. Soc. 84, 693.
Zhu, M., Carta, G., 2016. Protein adsorption equilibrium and kinetics in multimodal cation exchange resins. Adsorption 22, 165–179.